Periodic SIW Leaky-Wave Antenna With Large Circularly Polarized Beam Scanning Range

Yue-Long Lyu, *Student Member, IEEE*, Fan-Yi Meng, *Senior Member, IEEE*, Guo-Hui Yang, *Member, IEEE*, Daniel Erni, *Member, IEEE*, Qun Wu, *Senior Member, IEEE*, and Ke Wu, *Fellow, IEEE*

***Abstract*—In this letter, we propose and demonstrate a periodic leaky-wave antenna (P-LWA) by loading transverse slot pairs (TSPs) and longitudinal slots (LSs) along substrate integrated waveguide. The proposed P-LWA is able to yield a circularly polarized beam, which scans continuously from backward, through broadside, and to forward. Furthermore, it is shown that a large circularly polarized beam scanning range requires maximally coinciding radiation patterns of TSPs and LSs. Hence, within the design and optimization of the proposed P-LWA, the radiation pattern of the TSP should be adjusted to match the radiation pattern of the LS. A resulting large circularly polarized beam scanning range from $-40°$ to $25°$ has been predicted by simulations and experimentally verified. This circularly polarized beam scanning range turns out to be larger than in most of the previously reported works.**

***Index Terms*—Beam scanning, circular polarization, leaky-wave antenna, substrate integrated waveguide (SIW).**

I. Introduction

LEAKY-WAVE antennas (LWAs) have been widely investigated due to their simple feeding network, high radiating directivity, and frequency beam scanning property [1]. Especially, LWAs based on substrate integrated waveguide (SIW) have gained much attention for their low loss and easy integration with other planar circuits [2]. An LWA with periodic structure (P-LWA) is able to radiate electromagnetic (EM) power with high-order space harmonics. The P-LWA operating with the "-1"-order harmonic features beam scanning from backward, through broadside, and to forward [3]. However, many P-LWAs suffer from the stopband effect, which suppresses the broadside radiation. This stopband can be deliberately suppressed by several methods such as the impedance matching techniques [4]. However, most of the P-LWAs with continuous beam scanning from backward to forward are linearly polarized. Taking into account both continuous beam scanning and making circular polarization is a complex task to accomplish. Circularly polarized beam scanning can be obtained using two P-LWAs with orthogonal linear polarizations [2], [5]. This method is easy to implement but requires a relatively large area and an additional feed network. Circularly polarized P-LWA can also be realized through cascading radiating elements of orthogonal linear polarizations separated by $\pi/4$ delay lines [6], [7]. Furthermore, Otto *et al.* attribute the circularly polarized radiation of a P-LWA to axial asymmetric structure [8]. Actually, the mechanism of most circularly polarized P-LWAs [6]–[11] can be explained from this point of view. However, the circularly polarized radiation beam scanning range of such P-LWAs is usually limited. Although the axial ratio (AR) of a P-LWA can be optimized through adjusting the degree of axial asymmetry of the LWA [8], the reported circularly polarized beam scanning range is within $\pm 15°$.

In this letter, we propose an SIW P-LWA featuring both stopband effect suppression and circular polarization. A large circularly polarized beam scanning range is obtained by maximally coinciding radiation patterns of the series and shunt slots. A prototype is simulated, fabricated, and experimentally measured. A large circularly polarized radiation beam scanning range at least from $-40°$ to $25°$ is obtained.

II. Geometry of the Proposed P-LWA

The unit cell structure of the proposed P-LWA operating with -1 space-harmonic is shown in Fig. 1(a). The host TL of the proposed P-LWA is an SIW, made of a substrate (RO4350, $\varepsilon_r = 3.66$, $\tan\delta = 0.004$, and thickness $h_0 = 1.524$ mm) covered by copper on both sides with two rows of metallized via arrays. A transverse slot pair (TSP) and a longitudinal slot (LS) are etched on the top copper layer of the SIW. In this arrangement, TSP provides series radiation, while LS provides shunt radiation. The radiations of TSP and LS can be controlled independently, which makes the design and optimization procedure easy. The TSP and the LS topologies are arranged to be π-shaped as shown in Fig. 1(a) to achieve axial asymmetry for phase quadrature of the series and shunt radiation [8]. The total LWA (within the corresponding coordinate system) composed of cascaded unit cells is shown in Fig. 1(b).

As discussed in [4], for an SIW P-LWA with both transverse and longitudinal slots, the stopband at the transition frequency where the LWA radiates broadside can be suppressed by properly arranging the slots. After precise parameter optimization conducted in CST MWS, the final parameter values of the unit cell are given in the caption of Fig. 1. A P-LWA prototype

Manuscript received June 2, 2017; revised July 5, 2017; accepted July 7, 2017. Date of publication July 12, 2017; date of current version August 28, 2017. This work was supported by the National Nature Science Foundation of China under Grant 61671180 and Grant 61501275, by the Science Foundation Project of Heilongjiang Province of China under Grant QC2015073, and by the DFG CRC/TRR 196 MARIE. *(Corresponding author: Fan Yi Meng.)*

Y.-L. Lyu, F.-Y. Meng, G.-H. Yang, and Q. Wu are with the Department of Microwave Engineering, Harbin Institute of Technology, Harbin 150001, China (e-mail: lvyuelonglvyuelong@126.com; blade@hit.edu.cn; gh.yang@hit.edu.cn; qwu@hit.edu.cn).

D. Erni is with the Faculty of Engineering, Laboratory for General and Theoretical Electrical Engineering (ATE) and the Center for Nanointegration Duisburg–Essen (CENIDE), University of Duisburg–Essen, 47048 Duisburg, Germany (e-mail: daniel.erni@uni-due.de).

K. Wu is with the Poly-Grames Research Center, Polytechnique Montréal, Montréal, QC H3T 1J4, Canada (e-mail: ke.wu@polymtl.ca).

Color versions of one or more of the figures in this letter are available online at http://ieeexplore.ieee.org.

Digital Object Identifier 10.1109/LAWP.2017.2726089

1536-1225 © 2017 IEEE. Personal use is permitted, but republication/redistribution requires IEEE permission.
See http://www.ieee.org/publications_standards/publications/rights/index.html for more information.

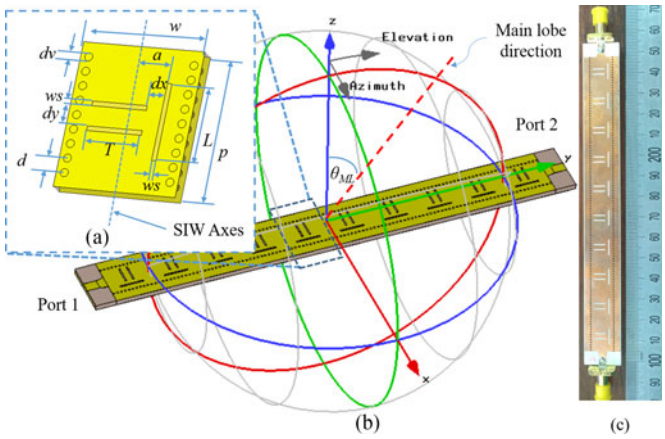

Fig. 1. Structure of the proposed LWA: (a) unit cell structure, (b) total LWA in the coordinates, and (c) prototype of the proposed LWA. Parameters are $w = 10.6$ mm, $a = 3$ mm, $d = 0.7$ mm, $dv = 0.4$ mm, $L = 7.4$ mm, $T = 5.4$ mm, $ws = 0.4$ mm, $p = 14$ mm, $dx = 1.5$ mm, and $dy = 2.4$ mm.

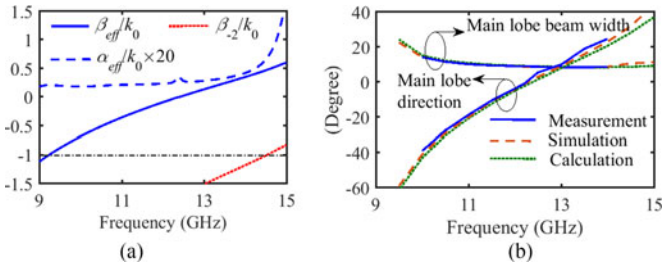

Fig. 2. (a) Simulated normalized dispersion diagram and (b) measured, simulated, and calculated main lobe direction and main lobe beamwidth.

consisting of ten cascaded units is simulated and fabricated [see Fig. 1(c)]. The normalized effective phase constant β_{eff}/k_0 and attenuation α_{eff}/k_0 are extracted through the ABCD matrix of unit cell as shown in Fig. 2(a) [4], and are used to calculate the main lobe direction and main lobe beamwidth [1] as shown in Fig. 2(b), where the simulated and measured results of the prototype are also depicted. β_{eff}/k_0 increases from negatively valued to positively valued continuously from 9 to 15 GHz, while α_{eff}/k_0 features only a small peak at 12.4 GHz, meaning that the stopband effect is well suppressed. The main lobe of the prototype scans from $-60°$ to $40°$, which is verified with the simulated and measured results. However, as shown in Fig. 2(a), the normalized phase constant of -2-order harmonic β_{-2}/k_0 is larger than -1 from 14.5 GHz, which means that the -1-order radiation is suppressed and the forward beam scanning range is limited due to the grating lobe caused by the -2-order radiation. Substrate with higher permittivity can be used to design the proposed unit cell to keep the -2-order radiation outside the -1-order radiation band. The backward beam scanning range is limited as the radiation efficiency of the proposed unit cell is low at the lower boundary of the operation band (as shown later in Fig. 8). The measured main lobe beamwidth of the prototype decreases from 12° to 8°, also agreeing well with the calculated and simulated results. The main lobe beamwidth of the prototype is stable over the whole frequency band.

The simulated and measured *S*-parameters are depicted in Fig. 3, where the measured and simulated results agree well with each other. The return loss of the P-LWA is larger than 10 dB

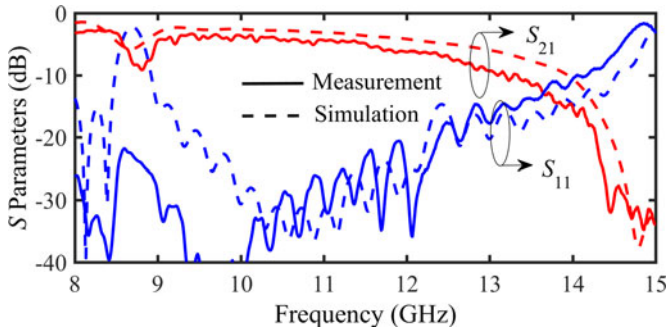

Fig. 3. Measured S-parameters of the proposed LWA compared to the simulated results.

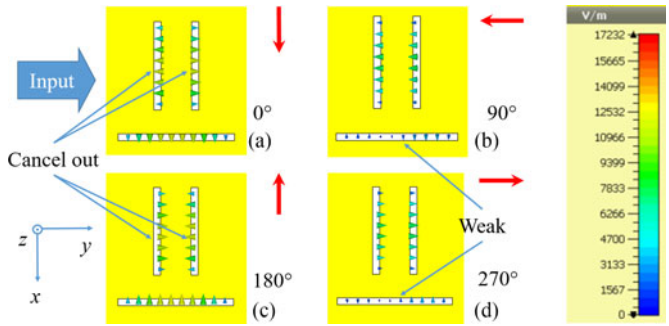

Fig. 4. Simulated electric field distribution of the unit cell at 12.4 GHz.

over the whole frequency band ranging from 9 to 14 GHz. Especially, $|S_{11}|$ around the transition frequency (12.4 GHz according to Fig. 2) is below -15 dB, which means the stopband effect is well suppressed. What is worth noting is that the stopband effect suppression of the unit cell should also take circularly polarized radiation optimization into account. If the optimized unit cell cannot effectively radiate a circularly polarized beam, the lengths and the arrangement of the slots should be correspondingly altered, and other parameters should also be adjusted to maintain a well-suppressed stopband.

III. Circularly Polarized Radiation and Its Optimization

The simulated electric fields on the top layer of the LWA unit cell with sequential phases at 12.4 GHz are illustrated in Fig. 4, where the EM power is fed into the unit cell from the left port and the residual power flows out of the unit cell from the right port. The net electric field (labeled by the red arrows in Fig. 4) point along the $+x$-axis, $-y$-axis, $-x$-axis, and $+y$-axis, successively. Therefore, the unit cell radiates EM power in the manner of a left-handed circular polarization (LHCP).

As mutual coupling between the adjacent unit cells is small, observing the simulated radiation patterns of a single unit cell is useful to optimize the circularly polarized beam scanning range of the total LWA. Once one unit cell maintains low AR in a large elevation angle range, the total LWA is able to radiate circularly polarized beam in a large elevation range. The simulated radiation patterns of LS in the *yoz* plane at different frequencies are depicted in Fig. 5(a). As frequency rises, LS radiates more EM power. Moreover, the maximum radiation of LS occurs in the forward region, which is rendered from the gradual field phase distribution along LS. The maximum radiation direction

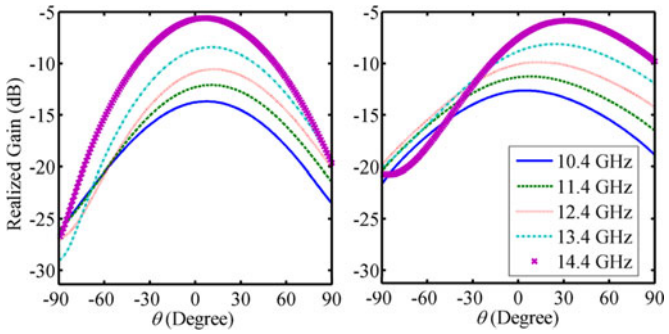

Fig. 5. Simulated radiation patterns of unit cell at different frequencies, where (a) is the radiation patterns of LS, and (b) is the radiation patterns of TSP.

of LS is 7° at 10.4 GHz, and stays at around 11° from 11.4 to 13.4 GHz, while lowering back to 6° at 14.4 GHz due to the frequency-dependent variation of phase distribution along LS. This frequency-dependent radiation brings a challenge in the design of a P-LWA with a large circularly polarized beam scanning range. Therefore, a series radiation with the same frequency dependence as the shunt radiation is necessary to enlarge the circularly polarized beam scanning range of a P-LWA, and series radiation components with frequency independence such as the single transverse slot used in [4] is not suitable. In the proposed design, the TSP with frequency scanning radiation pattern is used in the proposed unit cell as a proper measure.

In a TSP, as EM power travels through the two transverse slots successively, the two transverse slots radiate EM power with phase difference written as

$$\Delta\phi = \beta_{\mathrm{TL}} \cdot dy + \phi_T \tag{1}$$

where β_{TL} is the phase constant of TL between TSP, and ϕ_T is the phase delay caused by the EM power going through one transverse slot. With $t_0(\theta)$ denoting the normalized radiation pattern of a single transverse slot, the normalized radiation pattern of TSP in the *yoz* plane is expressed by

$$t(\theta) = \left|\cos\left(\left(\Delta\phi - k_0 dy \sin(\theta)\right)/2\right)\right| t_0(\theta) = t_d(\theta)\, t_0(\theta). \tag{2}$$

According to the empirical results, $t_0(\theta)$ is symmetrical with its maximum value at broadside of the unit cell. The other component of $t(\theta)$ is $t_d(\theta)$, which is mainly determined by $\Delta\phi$ because $k_0 dy \sin(\theta)$ is much smaller than $\Delta\phi$ especially near broadside. As $\Delta\phi$ varies with respect to frequency, the radiation pattern of TSP is also frequency-dependent. According to (1) and (2), the radiation pattern of TSP can be controlled by adjusting the distance dy between TSP and the length of the transverse slot T. In order to obtain the maximum overlap of the radiation patterns of LS and TSP in a large frequency band, the radiation pattern of TSP at the central frequency of the beam scanning band (transition frequency $f_0 = 12.4$ GHz) should be optimized to conform at the best to the LS radiation pattern. Fig. 5(b) depicts the simulated radiation patterns of TSP with the parameter values given in the caption of Fig. 1. The direction of the maximum radiation of TSP varies from 5° at 10.4 GHz to 32° at 14.4 GHz.

The simulated radiation patterns of LS and TSP of the unit cell at 12.4 GHz are illustrated in the same figure [see Fig. 6(a)] for comparison. It can be observed that the radiation patterns of LS and TSP are not totally identical, resulting in that the circularly polarized beam scanning range cannot cover the entire beam

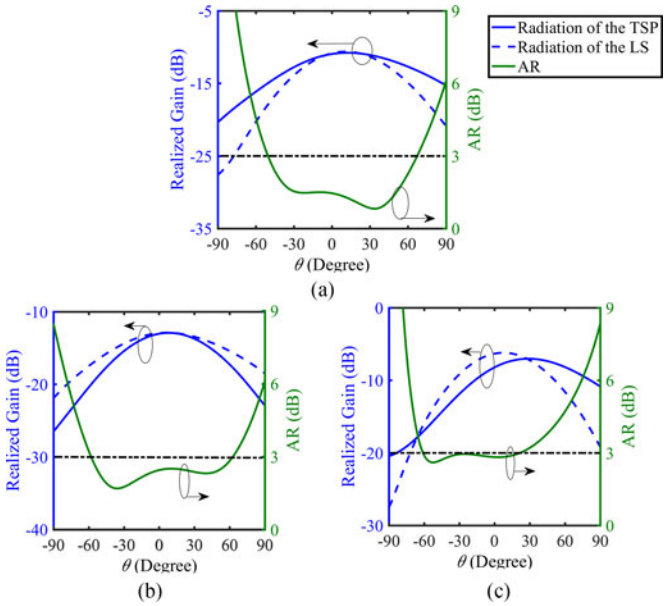

Fig. 6. Simulated radiation patterns and the AR of unit cell at (a) 12.4, (b) 11, and (c) 14 GHz.

scanning range of the P-LWA shown in Fig. 2(b). However, the two radiation patterns are similar within a large range of elevation angles centered on their maximum radiation angle. As a result, the AR, also depicted in Fig. 6(a), is below 3 dB from $-40°$ to $+60°$. This large angle range is necessary for a large circularly polarized beam scanning of the total LWA. The AR of the unit cell at broadside is 1.4 dB, which ensures the total LWA to radiate at broadside with circular polarization.

The radiation patterns and AR of the unit cell at 11 and 14 GHz are simulated and depicted in Fig. 6(b) and (c), respectively. In Fig. 6(b), the maximum radiation magnitude and the corresponding direction of TSP in the *yoz* plane still remain almost the same as those of LS because both the maximum radiation directions of TSP and LS shift backwardly as frequency decreases. Hence, AR in the backward angle range at 11 GHz is still below 3 dB, which ensures the circular polarization of the backwardly radiated beam of the total P-LWA. However, in higher frequency band, as frequency goes up, the maximum radiation direction of TSP scans forwardly, whereas the maximum radiation direction of LS moves back toward broadside. This discrepancy leads to a disagreement of the radiation patterns of TSP and LS as shown in Fig. 6(c) in the case of 14 GHz, and hence AR at this frequency deteriorates up to nearly 3 dB in the forward angle range, meaning that AR of the forward beam of the total P-LWA at 14 GHz cannot be as good as in the cases of 12.4 and 11 GHz. It should be noted that AR of the total P-LWA deteriorates slightly due to the small coupling between the adjacent unit cells, but the deterioration can be eliminated by slightly adjusting the length of the transverse slot T.

The LHCP (copolarization) and the right-handed circular polarization (RHCP) (cross-polarization) radiation patterns of the P-LWA prototype at 10, 12.3, and 14 GHz are measured and depicted in Fig. 7 together with simulated reference values. The measured radiation patterns at 10 and 12.3 GHz agree well with the simulated results. At 14 GHz, the measured cross-polarization level at 25° is higher than the simulated one, which deteriorates AR of the main lobe of the P-LWA prototype.

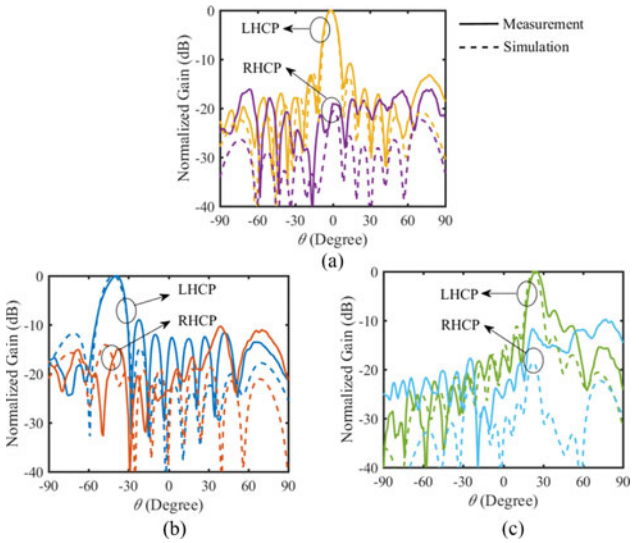

Fig. 7. Measured and simulated normalized LHCP (co-pol.) and RHCP (cross-pol.) radiation patterns of the prototype at (a) 12.3, (b) 10, and (c) 14 GHz.

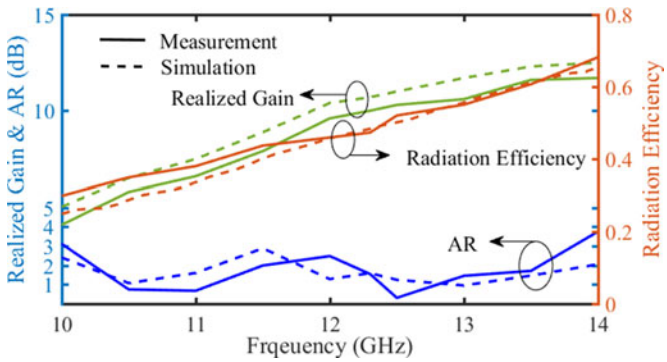

Fig. 8. Measured and simulated AR, realized gain, and radiation efficiency of the prototype.

The measured and simulated results of the realized gain and the radiation efficiency are depicted in Fig. 8. The measured gain has only a small deterioration compared to the simulated one. The measured radiation efficiency is calculated using the measured gain and the simulated directivity. The measured radiation efficiency is a little larger than the simulated one in the low-frequency band. As the total number of unit cell of the prototype is small, the EM power, especially at low frequencies of the -1-order radiation band, is not fully used to contribute to the radiation. Once the total number of unit cell is sufficiently increased, the radiation at lower frequency band can be enhanced more significantly than in higher frequency band, and hence the gain variation with respect to frequency will be suppressed.

The measured AR is depicted in Fig. 8 and shows a good agreement with the simulated results. The comparison of the circularly polarized beam scanning range of the proposed prototype and the recent published works are shown in Table I. The circularly polarized beam scanning range of the proposed prototype is notably wider than most of the previous works. Although the circularly polarized beam scanning range of the proposed prototype is smaller than that in [9], the proposed -1-order P-LWA features a broader backward radiation frequency band and a narrower main lobe beam especially in the backward radiation frequency band.

TABLE I
CIRCULARLY POLARIZED BEAM SCANNING RANGE COMPARISON

Ref. No.	Frequency Range (GHz)	Angle Range (Degree)	Percentage of Backward Radiation Bandwidth in the Total Operation Band
[10]	$10.3-11.6$	$+20-+50$	-
[8]	$23-25$	$-15-+15$	50%
[6]	$4.2-4.85$	$-29-+24$	38.5%
[9]	$7.4-13$	$-70-+70$	28.6%
This Work	$10-14$	$-40-+25$	60%

IV. CONCLUSION

In this letter, we propose an SIW-based -1-order periodic leaky-wave antenna with both transverse slot pairs and longitudinal slots. The proposed leaky-wave antenna radiates circularly polarized beam from backward and to forward continuously. Then, we point out that besides using axially asymmetrical structures, the coincidence between the radiation patterns of the series and shunt radiations becomes necessary to extend the circularly polarized beam scanning range. Therefore, the radiation pattern of TSP in the unit cell has been adjusted to provide the best possible overlap to the radiation pattern of longitudinal slot. Then, a prototype has been designed and fabricated, featuring a circularly polarized beam scanning range of $-40°-25°$, which is much wider than most of the scanning ranges reported in previous works.

REFERENCES

[1] A. A. Oliner and D. R. Jackson, *Antenna Engineering Hand Book*. 4th ed. New York, NY, USA: McGraw-Hill, 2007.
[2] Y. J. Cheng, W. Hong, and K. Wu, "Millimeter-wave half mode substrate integrated waveguide frequency scanning antenna with quadri-polarization," *IEEE Trans. Antennas Propag.*, vol. 58, no. 6, pp. 1848–1855, Jun. 2010.
[3] F. Xu and K. Wu, "Understanding leaky-wave structures: A special form of guided-wave structure," *IEEE Microw. Mag.*, vol. 14, no. 5, pp. 87–96, Jul./Aug. 2013.
[4] Y. L. Lyu *et al.*, "Leaky-wave antennas based on noncutoff substrate integrated waveguide supporting beam scanning from backward to forward," *IEEE Trans. Antennas Propag.*, vol. 64, no. 6, pp. 2155–2164, Jun. 2016.
[5] Y. Dong and T. Itoh, "Substrate integrated composite right-/left-handed leaky-wave structure for polarization-flexible antenna application," *IEEE Trans. Antennas Propag.*, vol. 60, no. 2, pp. 760–771, Feb. 2012.
[6] H. Lee, J. H. Choi, C. T. M. Wu, and T. Itoh, "A compact single radiator crlh-inspired circularly polarized leaky-wave antenna based on substrate-integrated waveguide," *IEEE Trans. Antennas Propag.*, vol. 63, no. 10, pp. 4566–4572, Oct. 2015.
[7] P. Sanchez-Olivares and J. L. Masa-Campos, "Novel four cross slot radiator with tuning vias for circularly polarized SIW linear array," *IEEE Trans. Antennas Propag.*, vol. 62, no. 4, pp. 2271–2275, Apr. 2014.
[8] S. Otto *et al.*, "Circular polarization of periodic leaky-wave antennas with axial asymmetry: Theoretical proof and experimental demonstration," *IEEE Trans. Antennas Propag.*, vol. 62, no. 4, pp. 1817–1829, Apr. 2014.
[9] A. P. Saghati, M. M. Mirsalehi, and M. H. Neshati, "A HMSIW circularly polarized leaky-wave antenna with backward, broadside, and forward radiation," *IEEE Antennas Wireless Propag. Lett.*, vol. 13, pp. 451–454, 2014.
[10] J. Liu, X. Tang, Y. Li, and Y. Long, "Substrate integrated waveguide leaky-wave antenna with H-shaped slots," *IEEE Trans. Antennas Propag.*, vol. 60, no. 8, pp. 3962–3967, Aug. 2012.
[11] P. Chen, W. Hong, Z. Kuai, and J. Xu, "A substrate integrated waveguide circular polarized slot radiator and its linear array," *IEEE Antennas Wireless Propag. Lett.*, vol. 8, pp. 120–123, 2009.